CrossMark

ORIGINAL ARTICLE

Removal of lead from aqueous solutions by a poly(acrylic acid)/bentonite nanocomposite

H. R. Rafiei · M. Shirvani · O. A. Ogunseitan

Abstract We synthesized a novel poly acrylic acid–organobentonite (PAA–Bent) nanocomposite by successive intercalation of cetyltrimethylammonium (CTA) surfactant and polyacrylic acid (PAA) into the bentonite (Bent) interlayer spaces. The surfactant-modified clay (CTA–Bent) and PAA–Bent nanocomposite were characterized by XRD and FT-IR techniques and used for removal of Pb(II) from aqueous solution. The XRD results confirmed the intercalation of CTA and PAA into the interlayer spaces of the bentonite increasing the d_{001} spacing of the clay from 12.2 up to 38.9 Å. FT-IR analysis of the modified clay samples revealed the functional groups of CTA and PAA constituents alighted on the bentonite surfaces. Maximum Pb sorption capacity of the Bent and PAA–Bent predicted by Langmuir model were 52.3 and 93.0 mg g^{-1}, respectively, showing that the synthesized nanocomposite superiorly adsorbed Pb from the solution as compared to the Bent. The maximum Pb removal efficiency of 99.6 % was achieved by the nanocomposite at 25 °C with <30 min contact time for a 7.5 g L^{-1} solid-to-liquid ratio and an initial metal concentration of 400 mg L^{-1}. The results indicated that PAA–Bent nanocomposite can be efficiently used as a superadsorbent for the removal of Pb(II) from aqueous solution.

Introduction

Lead (Pb) is one of the most toxic and easily encountered metals released into the environment through various industrial activities, consumer products, and waste disposal. Lead is used in the production of batteries, ammunition, sheet lead, solder, pipes, paints, medical equipment, ceramic glazes, and electronic products (Ogunseitan 2007; Hoet 2005). The two primary routes of Pb exposure for humans are inhalation and ingestion. After being absorbed from the gastrointestinal tract or the lungs into the blood system, Pb attaches to proteins in the blood and conducted to different tissues in the body (Ogunseitan et al. 2000; ATSDR 2007). Lead exposure is estimated to account for up to 3 % of the human burden of disease attributable to controllable environmental risk factors, and children are particularly vulnerable to the detrimental health impacts, including cognitive impairment, anemia, kidney malfunction, mental retardation, and cardiovascular disease (ATSDR 2007; Milovantseva and Ogunseitan 2011; Saleh and Gupta 2012).

Elevated levels of Pb in surface waters may be originated from deposits of atmospheric dust, industrial wastewater, urban runoff, and mine tailings (Chern et al. 2007). Removal of Pb from the polluted waters and wastewaters is, therefore, important in terms of protection of the public and environmental health. Traditional metal-removal techniques from water such as precipitation, oxidation, reduction, electrochemical treatment, reverse osmosis, solvent extraction, ion-exchange and evaporation are mostly expensive and difficult to apply (Özcan et al. 2009;

H. R. Rafiei · M. Shirvani (✉)
Department of Soil Science, College of Agriculture, Isfahan University of Technology, 84156-83111 Isfahan, Iran
e-mail: shirvani@cc.iut.ac.ir

O. A. Ogunseitan
Program in Public Health, Department of Population Health and Disease Prevention, University of California, Irvine, CA 92697-3957, USA

مدينة الملك عبدالعزيز
KACST للعلوم والتقنية

Springer

Kul and Koyuncu 2010; Gupta et al. 2012, Gupta and Rastogi 2009). Compared with the traditional methods, adsorption has received specific attention because it has significant advantages including high efficiency, easy handling, high selectivity and minimum production of chemical or biological sludge (Randelovic et al. 2012; Gupta et al. 2007a, b, 2009).

Clay minerals, polymers and activated carbon have been used as adsorbents for removing metals from aqueous solutions (Randelovic et al. 2012; Duranoglu et al. 2012). Activated carbon is the most extensively used adsorbent in water purification processes. However, it has some disadvantages including high cost, problems of regeneration, and difficulties of separation from wastewater (Wang et al. 2009a, b; Zhang et al. 2007). Recently, much attention has been paid to clay minerals such as bentonite (Zhao et al. 2010; Ulusoy and Simsek 2005; Futalan et al. 2011), attapulgite (Wang et al. 2009a, b; Chen and Wang 2009; Zhao et al. 2009), kaolinite (Unuabonah et al. 2008a, b) and zeolite (Ulusoy and Simsek 2005) as low-cost adsorbents with high specific surface area, chemical and mechanical stability, and high cation exchange capacities (CEC). Colloidal dispersions of clays, however, can cause some difficulties hindering water flow (Keren and Ben-Hur 2003).

Polymers, having numerous functional groups such as carboxylic, amine, hydroxyl and sulfonic, could be used as complexing agents for the adsorptive removal of metal ions from aqueous solutions (Futalan et al. 2011; Chen and Wang 2009; Bleiman and Mishael 2010). Lack of desirable mechanical properties and structural strength, however, is the main disadvantage of the most polymers for water treatment purposes. By intercalation of organic polymers into the layered clay galleries, organic–inorganic nanocomposites can be formed in which the clay framework serves to protect, stabilize and orient the polymer, and to mediate its function (Lu et al. 2001). For example, polyacrylic acid (PAA) possesses many polar carboxylic groups with ability to form strong complexes with metal ions in solution (Tran et al. 2005). The high water solubility of PAA, however, greatly hinders application of this polymer to remove heavy metal ions from wastewater. If PAA forms composites with clay particles, the solubility of the polymer becomes negligible as the polymer is linked to the insoluble clay particles. Furthermore, immobilization in the cross-linked network prevents coagulation of the dispersed clay particles.

Nanocomposite materials consisting of nanolayers of aluminosilicates and intercalated organic polymers have recently attracted considerable attention as potentially effective adsorbents. Few studies, however, have examined sorption of metal ions by the clay–polymer composites. For example, Chen and Wang (2009) synthesized a chitosan-g-poly(acrylic acid)/attapulgite composite for the removal of Cu(II) from aqueous solution. Huang et al. (2006) also developed cationic-modified zeolite microparticle/anionic polymer systems with great potential in wastewater treatments that require simultaneous removal of both soluble and colloidal contaminants. Here, we describe sorption abilities of a bentonite–polyacrylic acid nanocomposite for Pb(II) removal from aqueous solutions.

Materials and methods

Materials

All the chemicals used in this study were of analytical reagent grade and utilized without further purification. Bentonite (Bent) samples were collected from Mehredjan mine (33° 36′ 7″N, 55° 10′ 4″E), ground in a mortar and sieved using a no. 270 mesh (0.05 mm) sieve. The CEC of the bentonite sample was 66.0 cmol kg^{-1} as measured by Na-acetate method (Rhoades 1986).

A stock solution containing 2,000 mg of Pb(II) per liter was prepared by dissolving Pb(NO$_3$)$_2$ salt (Merck) in 0.01 M CaCl$_2$ and then diluting it to form various Pb concentrations between 50 and 1,200 mg L^{-1} for isothermal experiment. Cationic surfactant N-cetyltrimethylammonium (CTA) (bromide salt, purity >99 %) from Merck and poly acrylic acid (MWca. 2000) from Sigma-Aldrich was used in preparation of the nanocomposite.

Preparation of the organobentonite

An alkyl ammonium cation with long-chain (CTA$^+$) was used to widen the gallery spacing between platelets of the Bent, so that PAAs could be grafted into the modified clay. To prepare the CTA–Bent, 20 g natural Bent clay was mixed with 300 mL distilled water and 6 mL of HCl 0.01 M and the mixture was heated to 70 °C. The HCl was added into the clay suspension because acidic environment facilitates the distribution of quaternary ammonium cations inside the gallery spacing of the clays (Shirsath et al. 2011). Then, CTA solution (0.05 mol L^{-1}) was dispersed into the acidic Bent suspension. The amount of surfactant added was equal to 200 % of the clay CEC. The dispersion was subsequently stirred vigorously for 12 h at 70 °C. The organobentonite was washed repeatedly using hot water until a negative bromide test was obtained with 0.01 M of AgNO$_3$. The final precipitate was dried in an oven at 80 °C for 24 h followed by grinding and sieving through a 0.05-mm sieve.

Synthesis of PAA–Bent nanocomposite

The poly acrylic acid–bentonite nanocomposite (PAA–Bent) was prepared by dispersing 10 g of the CTA–Bent in 200 mL phosphate buffer solution (pH = 4.0) cooled to 4 °C and sonicated for 10 min. Then, 200 mL of a 5 % PAA aqueous solution was added to the reaction flask and the sonication was continued for 30 min at 4 °C. The mixture was then stirred at 60 °C for 3 h, centrifuged at 5,000 rpm for 20 min, and the sediment was dried in oven at 70 °C for 24 h. The dried sample was subsequently ground and particles smaller than 0.05 mm were used in the batch Pb(II) sorption studies.

Characterization of the modified clays

Organic carbon contents of the organobentonite samples were determined using a Skalar Primacs^{SLC} carbon analyzer to assess actual loading of the surfactant based on the percentage of the CEC occupied by organic cation.

X-ray powder diffraction (XRD) patterns of the Bent, CTA–Bent and PAA–Bent were obtained by a Philips PANalytical X'pert high score diffractometer using Cu Kα radiation ($\lambda = 1.5418$ Å at 40 kV and 40 mA) over the 2θ range of 2°–40°.

The surface functional groups of the samples were characterized by Fourier transform infrared spectroscopy (FT-IR). The samples for the FT-IR measurements were mounted on a JASCO FT-IR 460 spectrometer in KBr pellets at room temperature. FT-IR spectra were recorded in the range of 400–4,000 cm^{-1} with a resolution of 4 cm^{-1}. A Jasco Spectral Analysis version 1.53.04 was used for analyzing the spectral bands.

Lead sorption by the sorbents

Lead sorption tests were carried out using a batch technique. 0.15-g subsamples of each sorbent were transferred into 50-mL polyethylene centrifuge tubes in triplicates. Then, 20 mL of Pb(II) solutions in the concentration range of 50–1,200 mg L^{-1} was added to the tubes and the mixtures were agitated on a mechanical thermostatic shaker at 25 °C and 180 rpm for 24 h. After equilibration, the mixtures were centrifuged at 2,500 rpm for 10 min and concentration of Pb(II) in the supernatant was determined by a PerkinElmer AAnalyst 200 atomic absorption spectrophotometer (AAS). Sorption of Pb(II) on the centrifuge tube wall was negligible according to the sorption tests in the absence of the sorbents.

The effect of contact time on Pb(II) removal by the sorbents was also studied at 25 °C using a constant Pb(II) concentration of 400 mg L^{-1} in different times ranged from 5 to 1,440 min.

The sorbent dosage effect on Pb(II) removal was assessed by adding 20 mL volumes of an 800 mg Pb L^{-1} solution into 50-mL polyethylene centrifuge tubes containing 0.02, 0.05, 0.1, 0.15, 0.2 and 0.3 g of each sorbent. The reaction mixtures were then shaken at 25 °C for 24 h, centrifuged and concentration of Pb(II) in the supernatant was determined by the AAS. Blank samples without sorbent were also considered.

Data analysis

Equilibrium Pb(II) sorption on the sorbents at each concentration was calculated from the difference between initial and final Pb(II) concentrations using the Eq. (1):

$$q_i = \frac{(C_0 - C_i)V}{m} \tag{1}$$

where q_i is the equilibrium concentration of Pb(II) on the sorbent (mg g^{-1}), C_0 and C_i are the initial and equilibrium concentrations of Pb(II) in solution (mg L^{-1}), respectively, m is the mass of adsorbent (g) and V is the volume of the solution (L). The removal percentage of Pb ions from the solution was also calculated using the Eq. (2), as follows:

$$\%\text{Ads} = \frac{C_0 - C_i}{C_0} \times 100 \tag{2}$$

The equilibrium data were fitted to the Langmuir and Freundlich isotherm models using non-linear regression technique. The Langmuir isotherm model is as follows (Zhao et al. 2009):

$$q_i = \frac{q_{max}K_L C_i}{1 + K_L C_i} \tag{3}$$

where C_i and q_i are equilibrium concentrations of Pb(II) in solution (mg L^{-1}) and concentration of Pb(II) on the sorbent (mg g^{-1}), respectively, and q_{max} and K_L are the Langmuir constants related to the sorption capacity (mg g^{-1}) and affinity (L mg^{-1}), respectively.

The essential characteristic of the Langmuir equation can be expressed in terms of a dimensionless constant separation factor (R_L) (Chang et al. 2011), which is defined in Eq. (4):

$$R_L = \frac{1}{1 + K_L C_0} \tag{4}$$

where C_0 is the initial metal concentration (mg L^{-1}) and K_L is the Langmuir constant. The value of R_L indicates the nature of the sorption process to be either unfavorable ($R_L > 1$), linear ($R_L = 1$), favorable ($0 < R_L < 1$) or irreversible ($R_L = 0$) (Zhao et al. 2009).

The Freundlich model is as follows (Sheikhhosseini et al. 2013):

$$q_i = K_F C_i^N \tag{5}$$

where K_F is a sorption capacity index and N is a measure of strength of the adsorption process. The smaller the values of N, the stronger the sorption bond will be for that specific sorbate (US Environmental Protection Agency 2009).

Results and discussion

Surfactant loading of the organobentonite

The amount of CTA surfactant sorbed onto the Bent was determined from the organic carbon (OC) content of the CTA–Bent. The OC content of the original Bent was 0.05 % which increased to 27.81 % in case of the CTA–Bent. The amounts of CTA cations adsorbed by the Bent were, therefore, calculated from the OC content, being equivalent to about 185 % of the CEC of the clay. Also, the OC content of the PAA–Bent was greater than that of the CTA–Bent, suggesting that the PAA reacted successfully with the CTA–Bent.

XRD patterns

The X-ray diffraction (XRD) patterns of the Bent, CTAB–Bent and PAA–Bent are presented in Fig. 1, showing that the Bent mainly consisted of montmorillonite. Shift of the 001 peak of the montmorillonite toward the lower diffraction angles (2θ) is a suitable indicator of increasing interlayer spacing (d_{001}) of the clay. Montmorillonite showed a d_{001}-spacing of 12.2 Å which corresponds to an interlayer space (D) of 2.6 Å ($D = 12.2 - 9.6 = 2.6$ Å, where 9.6 Å is the thickness of the individual clay layer). The basal spacing d_{001} increased to 35.5 Å in the case of
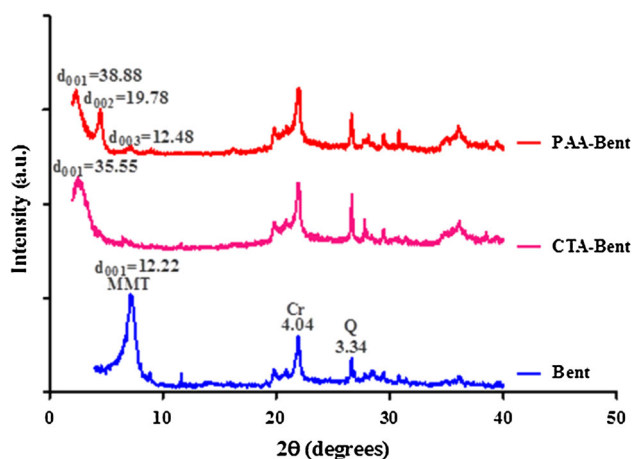
Table 1 FT-IR vibration band positions and their assignments for Bent, CTA–Bent, PAA–Bent, CTA and PAA

Assignment	Band position (cm^{-1})				
	Bent	CTAB	CTA–Bent	PAA	PAA–Bent
Si–O–Si bending vibrations	469.58	–	466.69	–	467.65
Si–O–Al bending vibrations	520.68	–	519.72	–	519.72
Si–O–Si stretching vibration	1040.41	–	1038.48	–	1039.44
Si–O– vibration	1093.44	–	1093.44	–	1090.55
H–O–H bending vibration	1637.27	–	1637.27	–	–
C=O stretching vibration	–	–	–	1647.87	1671.98
Symmetric C–H stretching vibration	–	2849.31	2850.27	–	2851.24
Asymmetric C–H stretching vibration	–	2917.77	2919.7	–	2921.63
H–O–H stretching vibration (for H$_2$O)	3435.56	–	3434.6	–	3433.64
Stretching vibrations of inner Al(OH) groups	–	–	3620.7	–	3620.7

the CTA–Bent organo-clay with corresponding interlayer space of 25.95 Å which is attributed to the intercalation of long-chain cationic surfactant into the interlayer of montmorillonite, forming the intercalated nanostructure (Wang and Wang 2008; Mishra et al. 2012).

The orientation of the surfactant ions in the montmorillonite interlayer space probably is a solid-like paraffinic arrangement of the chains with high packing density (Giannakas et al. 2008). Koswojo et al. (2010) also reported that, after modification process of a bentonite sample with CTA equivalent to 150 % of the clay CEC, basal spacing was increased to 25.1 Å. In practice, surface modification of montmorillonite is required prior to the polymer nanocomposite synthesis (Tran et al. 2005; Huang et al. 2006). The role of the surfactant is mainly to enlarge the interlayer spacing to make room for the polymer to penetrate into the gallery space during the preparation of polymer–clay nanocomposites (Giannakas et al. 2008; Janković et al. 2011).

The basal spacing of the PAA–Bent was 38.8 Å, indicating intercalation of the polymer into the interlayer space of the organobentonite. For PAA–Bent nanocomposite, the d_{002} and d_{003} reflections were also clearly shown in the XRD pattern (Fig. 1) indicating a highly ordered structure of the nanocomposite (Giannakas et al. 2008).

Fig. 1 XRD diffractograms of bentonite (Bent), CTA surfactant-modified bentonite (CTA–Bent) and polyacrylic acid–organobentonite nanocomposite (PAA–Bent)

FT-IR evidences

The FT-IR results of the Bent, CTA, CTA–Bent, PAA and PAA–Bent are represented in Table 1. The characteristic absorption bands of the symmetric and asymmetric stretching vibrations of the –CH$_2$ (2,850 cm^{-1}) and –CH$_3$ (2,919 cm^{-1}), and the bending vibrations of –CH$_3$ (1,468 cm^{-1}) related to the CTA surfactant (Wang and Wang 2008; Bakhtiary et al. 2013) were observed on the FT-IR spectra of the surfactant-modified bentonite confirming the adsorption/intercalation of the CTA cations into the montmorillonite galleries.

The absorption bands related to bending vibrations of Si–O–Si and Si–O–Al occurred at 469.6 and 520.7 cm^{-1}, respectively (Zohra et al. 2008), but the position of the bands was slightly changed to lower wave numbers after modification of bentonite with CTA surfactant (Table 1). The absorption peak at 1,671.9 cm^{-1} in the spectrum of the nanocomposite was attributed to the C=O stretching vibrations of the COOH group (Zhao et al. 2009; Mahmoud et al. 2011), indicating successful grafting of PAA on the surface of the CTA–Bent.

Lead sorption isotherms

The Pb(II) sorption parameters and correlation coefficients obtained from the Langmuir and Freundlich equations fitted to the sorption data are listed in Table 2. The maximum Pb(II) sorption capacity of the Bent at 25 °C was 52 mg g^{-1} which increased to 93 mg g^{-1} for the PAA–Bent system showing that the polymer–clay nanocomposite has much greater capacity for removal of Pb(II) from water as compared to the natural bentonite. The sorption capacity of Pb(II) by the CTA–Bent was 37 mg g^{-1} which was smaller than those of the PAA–Bent and even Bent. The Freundlich K_F constant, which is a measure of sorption capacity, was also greater for PAA–Bent than Bent which is in accordance with the q_{max} values obtained from the Langmuir model. Table 3 compares Pb(II) sorption capacities of different sorbents reported in the literature with that of the nanocomposite obtained in this study. Although it is difficult to compare the sorption capacities determined in different experimental conditions, the PAA–Bent possesses a relatively high capacity for Pb(II).

The Langmuir K_L constant was 0.128 and 0.226 L g^{-1} for the Bent and PAA–Bent samples indicating that the affinity of the nanocomposite for binding of Pb(II) ions is more than that of the Bent. The values of Freundlich N parameter were 0.202 and 0.172 for Bent and PAA–Bent, respectively (Table 2), which indicates Pb(II) forms stronger bonds with the nanocomposite functional groups as the smaller Freundlich N values show the stronger bonds (US Environmental Protection Agency 2009). Superior capacity and affinity of PAA–Bent nanocomposite toward Pb(II) are probably due to complex formation between the polymer carboxyl groups and Pb ions as well as development of sorption spaces as a result of the clay expansion.

Table 2 Langmuir and Freundlich isotherm parameters for Pb(II) sorption data on bentonite (Bent) and poly acrylic acid–organobentonite nanocomposite (PAA–Bent) at 25 °C

Sorbent	Langmuir				Freundlich		
	q_{max} (mg g^{-1})	K_L (L mg^{-1})	r^2	R_L	K_F	N	r^2
PAA–Bent	93.01	0.226	0.943	0.080–0.003	33.77	0.172	0.897
Bent	52.31	0.168	0.862	0.105–0.004	15.39	0.209	0.963

Table 3 Comparison of Pb(II) sorption capacities of various sorbents with that of the PAA–Bent nanocomposite obtained in the current study
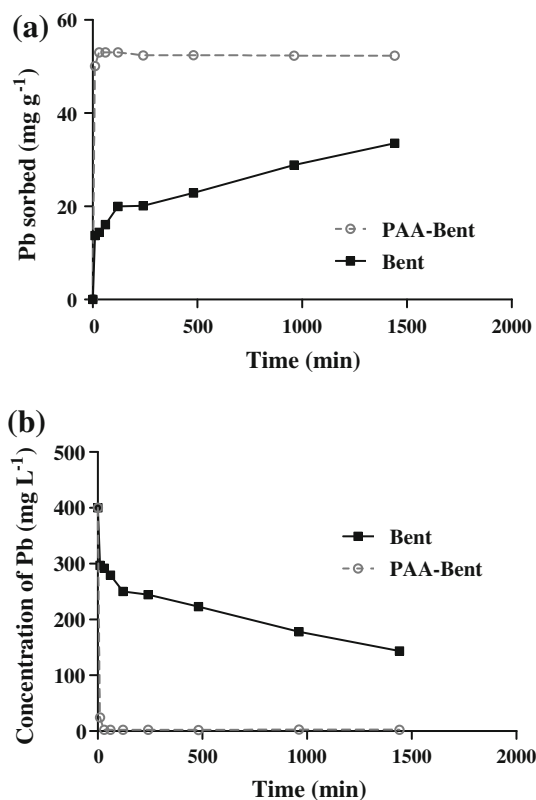
Sorbent	q_{max} (mg g^{-1})	Temp. (K)	References
Multi-walled carbon nanotubes	17.5	293	Ren et al. (2011)
Activated carbon	21.80	303	Rao et al. (2009)
8-Hydroxy quinoline-immobilized bentonite	142.94	323	Özcan et al. (2009)
Clay–poly(methoxyethyl)acrylamide	81.02	323	Sölener et al. (2008)
Sodium tetraborate-modified kaolinite clay	56.18	323	Unuabonah et al. (2008a, b)
Tetrabutylammonium-montmorillonite	30.67	303	Gupta and Bhattacharyya (2005)
Acid activated bentonite	2.31	328	Kul and Koyuncu (2010)
Magnesium oxide-coated bentonite	31.86	295	Eren (2009)
Amino-functionalized magnetic nanoadsorbent	40.10	298	Tan et al. (2012)
Polyacrylic acid–organobentonite nanocomposite	93	298	This work

The separation factor (R_L) values were all below 1.0 (Table 2), which indicate the favorable adsorption of Pb(II) by Bent and PAA–Bent; however, the superior q_{max} and K_L values indicate that PAA–Bent exhibits an excellent potential for adsorption of Pb(II) from aqueous solutions.

Effect of time on Pb(II) sorption

The Pb(II) sorption from aqueous solution by Bent and PAA–Bent as a function of contact time is shown in Fig. 2a. The sorption of Pb(II) ions onto PAA–Bent nanocomposite was very fast and reached a pseudo-equilibrium within 30 min. This may be due to the great capacity of the nanocomposite with numerous reactive carboxyl functional groups on the surface for complexation of Pb(II) ions. It can be seen in Fig. 2b that Pb(II) concentration decreased sharply from 400 mg L^{-1} to about 1.5 mg L^{-1} within 30 min which is less than the discharge limit for wastewater (Karatas 2012). The corresponding Pb(II) removal by the nanocomposite was 99.6 % which was significantly greater than the 63.62 % removal by the Bent. Sorption of Pb(II) on the Bent also started with an initial rapid step followed by a slower one, but no pseudo-equilibrium condition was reached within 24 h. The Bent
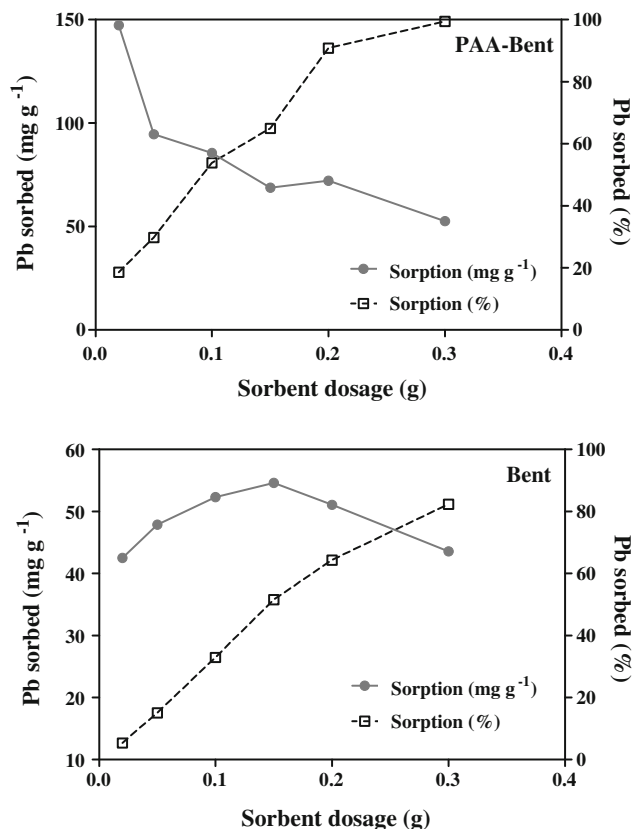
sample partly reduced Pb concentration in solution from 400 to 143.6 mg L^{-1} after 24 h. Tan et al. (2012) reported that rapid Pb adsorption on functionalized Fe_3O_4 magnetic nanoparticles which occurred during the early stage may be due to the abundant availability of active sites on the adsorbents. With gradual decrease in the number of active sites, however, the uptake of Pb(II) ions became very slow.

Effect of sorbent dosage on Pb(II) sorption

The effect of sorbent dosage on the removal of Pb(II) ions by the Bent and PAA–Bent is presented in Fig. 3. With increasing the sorbent dosage from 0.02 to 0.3 g, the percentage of the Pb(II) removal increased from 5.35 to 82.31 % by the Bent and from 18.45 to 99.43 % for PAA–Bent nanocomposite. This trend is related to the larger number of binding sites for Pb(II) ions in the systems containing larger dosages of sorbent. The maximum Pb(II) removal from the solution was attained using PAA–Bent with dose of 0.3 g which decreased the Pb(II) concentration from 800 to 4.53 mg L^{-1}. However, the amount of Pb(II) sorbed per unit mass of the Bent or PAA–Bent samples reduced with increasing the sorbent

Fig. 2 Effect of sorption time on Pb(II) sorption (a) and Pb(II) remaining concentration in solution (b) (concentration of Pb solution 400 mg L^{-1}, sorbent dosage 0.15 g, 20 mL Pb(II) solution)

Fig. 3 Effect of sorbent dosage on removal of Pb(II) by Bent and PAA–Bent from 20 mL aqueous solutions containing initial Pb concentration of 800 mg L^{-1} at 25 °C

dosage. This phenomenon has been previously reported by other researchers and ascribed to the interaction between colloidal particles (Gupta et al. 2007a, b; 2010; Wang et al. 2009a, b). At the same sorbent dosage, the amount of Pb(II) sorbed per unit mass of PAA–Bent was greater than that for the Bent which can be explained by the fact that PAA–Bent contains larger numbers of adsorption sites (carboxyl functional groups) on its surface as compared to the Bent.

Conclusion

In this study, a polyacrylic acid–organobentonite nanocomposite (PAA–Bent) was synthesized, characterized and its performance was tested for the sorption of Pb(II) ions from aqueous solutions. XRD diffractograms showed that CTA surfactant cations and PAA polymers entered the interlayer of montmorillonite, the major mineral phase present in the Bent sample, resulting in formation of an intercalated nanostructure. FT-IR also revealed the specific functional groups belonging to the CTA and PAA constituents adsorbed and intercalated into the montmorillonite galleries. The maximum sorption capacity of the nanocomposite was 93 mg g^{-1} which was approximately twice as much as that of untreated Bent (52 mg g^{-1}). The results also showed that PAA–Bent sorbed Pb very rapidly and a pseudo-equilibrium condition reached within 30 min. It can be concluded that PAA–Bent nanocomposite represents a new sorbent for efficient and fast removal of Pb ions from aqueous solutions, which may contribute to the improvement of waste water treatment and storm water filtration at the urban/watershed interface (Hipp et al. 2006).

References

Agency for Toxic Substances and Disease Registry (ATSDR) (2007) Toxicological profile for lead. U.S. Department of Health and Human Services, Atlanta

Bakhtiary S, Shirvani M, Shariatmadari H (2013) Characterization and 2,4-D adsorption of sepiolite nanofibers modified by *N*-cetylpyridinium cations. Microporous Mesoporous Mater 168:30–36

Bleiman N, Mishael YG (2010) Selenium removal from drinking water by adsorption to chitosan–clay composites and oxides: batch and columns tests. J Hazard Mater 183:590–595

Chang Y, Liu H, Zha F, Chen H, Ren X, Lei Z (2011) Adsorption of Pb(II) by *N*-methylimidazole modified palygorskite. Chem Eng J 167:183–189

Chen H, Wang A (2009) Adsorption characteristics of Cu(II) from aqueous solution onto poly(acrylamide)/attapulgite composite. J Hazard Mater 165:223–231

Chern EC, Tsai DW, Ogunseitan OA (2007) Deposition of glomalin-related soil proteins and sequestered toxic metals into watersheds. Environ Sci Technol 42:3566–3572

Duranoglu D, Kaya IGB, Beker U, Senkal BF (2012) Synthesis and adsorption properties of polymeric and polymer-based hybrid adsorbent for hexavalent chromium removal. Chem Eng J 181–182:103–112

Eren E (2009) Removal of lead ions by Unye (Turkey) bentonite in iron and magnesium oxide-coated forms. J Hazard Mater 165:63–70

Futalan CM, Kan C, Dalida ML, Hsien K, Pascua C, Wan M (2011) Comparative and competitive adsorption of copper, lead, and nickel using chitosan immobilized on bentonite. Carbohydr Polym 83:528–536

Giannakas A, Spanos CG, Kourkoumelis N, Vaimakis T, Ladavos A (2008) Preparation, characterization and water barrier properties of PS/organo-montmorillonite nanocomposites. Eur Polym J 44:3915–3921

Gupta SS, Bhattacharyya KG (2005) Interaction of metal ions with clays: I. A case study with Pb(II). Appl Clay Sci 30:199–208

Gupta VK, Rastogi A (2009) Biosorption of hexavalent chromium by raw and acid-treated green alga *Oedogonium hatei* from aqueous solutions. J Hazard Mater 163:396–402

Gupta VK, Jain R, Varshney S (2007a) Removal of Reactofix golden yellow 3 RFN from aqueous solution using wheat husk—an agricultural waste. J Hazard Mater 142:443–448

Gupta VK, Ali I, Saini VK (2007b) Defluoridation of wastewaters using waste carbon slurry. Water Res 41:3307–3316

Gupta VK, Mittal A, Malviya A, Mittal J (2009) Adsorption of carmoisine A from wastewater using waste materials—bottom ash and deoiled soya. J Colloid Interface Sci 335:24–33

Gupta VK, Rastogi A, Nayak A (2010) Biosorption of nickel onto treated alga (*Oedogonium hatei*): application of isotherm and kinetic models. J Colloid Interface Sci 342:533–539

Gupta VK, Ali I, Tawfik AS, Nayak A, Agarwal S (2012) Chemical treatment technologies for waste-water recycling—an overview. RSC Adv 2:6380–6388

Hipp A, Ogunseitan OA, Lejano R, Smith CS (2006) Optimization of stormwater filtration at the urban/watershed interface. Environ Sci Technol l40:4794–4801

Hoet P (2005) Speciation of lead in occupational exposure and clinical health aspects. In: Cornelis R, Caruso J, Crews H, Heumann K (eds) Handbook of elemental speciation, II-species in the environment, food, medicine and occupational health. Wiley, Chichester, pp 252–276

Huang L, Xiao H, Ni Y (2006) Cationic-modified microporous zeolites/anionic polymer system for simultaneous removal of dissolved and colloidal substances from wastewater. Sep Purif Technol 49:264–270

Jankovič L, Madejová J, Komadel P, ková DJ, Chodák I (2011) Characterization of systematically selected organo-montmorillonites for polymer nanocomposites. Appl Clay Sci 51:438–444

Karatas M (2012) Removal of Pb(II) from water by natural zeolitic tuff: kinetics and thermodynamics. J Hazard Mater 199–200:383–389

Keren R, Ben-Hur M (2003) Interaction effects of clay swelling and dispersion and CaCO$_3$ content on saturated hydraulic conductivity. Soil Res 41:979–989

Koswojo R, Utomo RP, Ju Y, Ayucitra A, Oetaredjo FE, Sunarso J, Ismadji S (2010) Acid Green 25 removal from wastewater by organo-bentonite from Pacitan. Appl Clay Sci 48:81–86

Kul AR, Koyuncu H (2010) Adsorption of Pb(II) ions from aqueous solution by native and activated bentonite: kinetic, equilibrium and thermodynamic study. J Hazard Mater 179:332–339

Lu Y, Yang Y, Sellinger A, Lu M, Huang J, Fan H, Haddad R et al (2001) Self-assembly of mesoscopically ordered chromatic polydiacetylene/silica nanocomposites. Nature 410:913–917

Mahmoud ME, Osman MM, Ahmed SB, Abdel-Fattah TM (2011) Improved adsorptive removal of cadmium from water by hybrid chemically and biologically carbonaceous sorbents. Chem Eng J 175:84–94

Milovantseva N, Ogunseitan OA (2011) Composite measures of environmental burden of disease at the global level. In: Nriagu J (ed) Encyclopedia of environmental health. Elsevier, Oxford, pp 813–821

Mishra AK, Allauddin S, Narayan R, Aminabhavi TM, Raju KVSN (2012) Characterization of surface-modified montmorillonite nanocomposites. Ceram Int 38:929–934

Ogunseitan OA (2007) Public health and environmental benefits of adopting lead-free solders. JOM 59:12–17

Ogunseitan OA, Yang S, Ericson JE (2000) Microbial delta-amino-levulinate dehydratase as a biosensor of lead (Pb) bioavailability in contaminated environments. Soil Biol Biochem 32:1899–1906

Özcan AS, Gök O, Özcan A (2009) Adsorption of lead(II) ions onto 8-hydroxy quinoline-immobilized bentonite. J Hazard Mater 161:499–509

Randelovic M, Purenovic M, Zarubica A, Purenovic J, Matovic B, Momcilovic M (2012) Synthesis of composite by application of mixed Fe, Mg (hydr)oxides coatings onto bentonite—a use for the removal of Pb(II) from water. J Hazard Mater 199–200:367–374

Rao MM, Ramana DK, Seshaiah K, Wang MC, Chien SWC (2009) Removal of some metal ions by activated carbon prepared from *Phaseolus aureus hulls*. J Hazard Mater 166:1006–1013

Ren X, Shao D, Yang S, Hu J, Sheng G, Tan X, Wang X (2011) Comparative study of Pb(II) sorption on XC-72 carbon and multi-walled carbon nanotubes from aqueous solutions. Chem Eng J 170:170–177

Rhoades JW (1986) Cation exchange capacity. In: Page CA (ed) Methods of soil analysis. ASA Press, Madison, pp 149–158

Saleh TA, Gupta VK (2012) Column with CNT/magnesium oxide composite for lead(II) removal from water. Environ Sci Pollut Res 19:1224–1228

Sheikhhosseini A, Shirvani M, Shariatmadari H (2013) Competitive sorption of nickel, cadmium, zinc and copper on palygorskite and sepiolite silicate clay minerals. Geoderma 192:249–253

Shirsath SR, Hage AP, Zhou M, Sonawane SH, Ashokkumar M (2011) Ultrasound assisted preparation of nanoclay Bentonite-FeCo nanocomposite hybrid hydrogel: a potential responsive sorbent for removal of organic pollutant from water. Desalination 281:429–437

Sölener M, Tunali S, Özcan AS, Özcan A, Gedikbey T (2008) Adsorption characteristics of lead(II) ions onto the clay/poly(methoxyethyl)acrylamide (PMEA) composite from aqueous solutions. Desalination 223:308–322

Tan Y, Chen M, Hao Y (2012) High efficient removal of Pb (II) by amino-functionalized Fe_3O_4 magnetic nano-particles. Chem Eng J 191:104–111

Tran NH, Dennis GR, Milev AS, Kannangara GSK, Wilson MA, Lamb RN (2005) Interactions of sodium montmorillonite with poly(acrylic acid). J Colloid Interface Sci 290:392–396

Ulusoy U, Simsek S (2005) Lead removal by polyacrylamide-bentonite and zeolite composites: effect of phytic acid immobilization. J Hazard Mater B127:163–171

Unuabonah EI, Adebowale KO, Olu-Owolabi BI, Yang LZ (2008a) Comparison of sorption of Pb^{2+} and Cd^{2+} on Kaolinite clay and polyvinyl alcohol-modified Kaolinite clay. Adsorption 14:791–803

Unuabonah EI, Adebowale KO, Olu-Owolabi BI, Yang LZ, Kong LX (2008b) Adsorption of Pb (II) and Cd (II) from aqueous solutions onto sodium tetraborate-modified Kaolinite clay: equilibrium and thermodynamic studies. Hydrometallurgy 93:1–9

US Environmental Protection Agency (2009) Drinking water treatability database, GAC, isotherm. US Environmental Protection Agency, Cincinnati

Wang L, Wang A (2008) Adsorption properties of Congo Red from aqueous solution onto surfactant-modified montmorillonite. J Hazard Mater 160:173–180

Wang X, Zheng Y, Wang A (2009a) Fast removal of copper ions from aqueous solution by chitosan-g-poly(acrylic acid)/attapulgite composites. J Hazard Mater 168:970–977

Wang Y, Tang X, Chen Y, Zhan L, Li Z, Tang Q (2009b) Adsorption behavior and mechanism of Cd(II) on loess soil from China. J Hazard Mater 172:30–37

Zhang G, Qu J, Liu H, Cooper AT, Wu R (2007) $CuFe_2O_4$/activated carbon composite: a novel magnetic adsorbent for the removal of acid orange II and catalytic regeneration. Chemosphere 68:1058–1066

Zhao Y, Chen Y, Li M, Zhou S, Xue A, Xing W (2009) Adsorption of Hg^{2+} from aqueous solution onto polyacrylamide/attapulgite. J Hazard Mater 171:640–646

Zhao G, Zhang H, Fan Q, Ren X, Li J, Chen Y, Wang X (2010) Sorption of copper(II) onto super-adsorbent of bentonite-poly-acrylamide composites. J Hazard Mater 173:661–668

Zohra B, Aicha K, Fatima S, Nourredine B, Zoubir D (2008) Adsorption of Direct Red 2 on bentonite modified by cetyltri-methylammonium bromide. Chem Eng J 136:295–305